

# A comparison of molecular hyperpolarizabilities from gas and liquid phase measurements

Philip Kaatz, Elizabeth A. Donley,<sup>a)</sup> and David P. Shelton<sup>b)</sup>  
*Department of Physics, University of Nevada Las Vegas, Las Vegas, Nevada 89154-4002*

(Received 4 August 1997; accepted 10 October 1997)

The first and second hyperpolarizabilities ( $\beta$  and  $\gamma$ ) of eight molecules at a fundamental wavelength of 1064 were measured by gas-phase electric-field-induced second-harmonic generation (EFISH), gas-phase hyper-Rayleigh scattering (HRS), and liquid-phase HRS experiments. The EFISH measurements give accurate values of  $\beta$  and  $\gamma$  for these molecules in the gas phase, and the HRS measurements show that the effective  $\beta$  of these molecules in the liquid is enhanced over the gas-phase value by a factor which varies from  $\approx 0.4$  to 2.0, over and above the Lorentz local field factors. Combining all of the measurements provides an accurate, absolute determination of the effective  $\beta$  for HRS in the liquid phase. The results for  $\text{CCl}_4$ , suitable as reference standards, are  $\langle \beta_{VV}^2 \rangle^{1/2} = 18.6 \pm 0.7$  au in the liquid phase and  $\beta_{xyz} = 20.7 \pm 1.6$  au in the gas phase. Comparison of measurements between hydrogenated and deuterated molecules indicates that vibrational contributions to  $\beta$  are small. © 1998 American Institute of Physics. [S0021-9606(98)03203-6]

## I. INTRODUCTION

Hyper-Rayleigh (HRS) or second-harmonic light scattering measurements have become an important method for measuring first hyperpolarizabilities  $\beta$  of organic chromophores.<sup>1-3</sup> This technique is more flexible and much simpler than electric-field-induced second-harmonic generation (EFISH), which is the principal alternative method for determining  $\beta$ . However, unresolved difficulties with the absolute calibration of solution EFISH measurements have not been avoided,<sup>4</sup> but only compounded, because uncertain EFISH values are typically used to calibrate the HRS measurements, and because different combinations of tensor components are measured in the two experiments. Furthermore, HRS signals from molecular liquids can include large intermolecular contributions, which have usually been ignored, although in fact they may dominate the nonlinear light scattering intensity.<sup>5</sup> These systematic problems impede a critical comparison of experimentally and theoretically determined molecular hyperpolarizabilities.

To address these issues, we have made gas-phase EFISH, gas-phase HRS, and liquid-phase HRS measurements of  $\beta$  for several molecules, all at a fundamental wavelength  $\lambda_\omega = 1064$  nm. Gas-phase EFISH measurements are a well-established means for determining accurate absolute molecular hyperpolarizabilities. Combining such gas-phase EFISH hyperpolarizabilities with supplementary information about tensor component ratios, one obtains accurate gas-phase HRS hyperpolarizabilities. Then, using the gas-phase HRS  $\beta$  for calibration, the effective liquid-phase HRS  $\beta$  can be determined from measurements of the relative intensity of HRS from gas- and liquid-phase samples. This procedure gives the effective  $\beta$  of a molecule in the liquid phase, based on an absolute gas-phase calibration for the same molecule.

In the following, the results of this program of experimental measurements for several molecules are presented, critically assessed, and compared with previous measurements and with theoretical *ab initio* calculations of molecular hyperpolarizabilities.

## II. THEORY

The theory of the gas-phase EFISH measurement has been discussed many times, see, e.g., Willetts *et al.*<sup>4</sup> or Shelton and Rice<sup>6</sup> and references therein. As experimentalists and theorists sometimes differ in the definition of the measured quantities, we briefly describe the conventions adopted in this work. The EFISH experiment provides a measure of the third-order nonlinear susceptibility,  $\chi^{(3)}(-2\omega; \omega, \omega, 0)$ , which is directly related to the thermally averaged microscopic second hyperpolarizability  $\Gamma$ ,

$$\chi^{(3)}(-2\omega; \omega, \omega, 0) = \frac{1}{4} \mathcal{L}_\omega \mathcal{L}_\omega^2 \mathcal{L}_{2\omega} \rho \Gamma, \quad (1)$$

where  $\mathcal{L}_\omega$  is the Lorentz local field factor at frequency  $\omega$ , and  $\rho$  is the molecular number density. In the case of a dipolar molecule in the presence of static and optical electric fields with parallel polarizations,  $\Gamma$  is described by the following expression:

$$\Gamma = \gamma + \frac{\mu_0 \beta_{\parallel}}{3kT}, \quad (2)$$

where  $\gamma$  is the scalar component of the second hyperpolarizability,  $\mu_0$  is the static dipole moment,  $k$  is Boltzmann's constant,  $T$  is the temperature, and  $\beta_{\parallel}$  denotes the component of  $\beta$  in the direction of the dipole moment and can be written in terms of the components of  $\beta$  as

$$\beta_{\parallel} = \frac{1}{5} \sum_i (\beta_{zii} + \beta_{izi} + \beta_{iiz}) = \frac{3}{5} \beta_z. \quad (3)$$

<sup>a)</sup>Present address: Physical Chemistry Laboratory, Swiss Federal Institute of Technology (ETH), CH-8092 Zürich, Switzerland.

<sup>b)</sup>Electronic mail: shelton@physics.unlv.edu

Some experimentalists use  $\beta_z$  in Eq. (2), in which case the numerical factor is 5 rather than 3. Other conventions are also used in the EFISH experiment for the definitions of the molecular hyperpolarizabilities.<sup>4</sup>

HRS differs from EFISH in that the observed signal is the result of the incoherent addition of second-harmonic light scattered from regions of molecular dimensions, whereas the EFISH signal is coherent forward scattering due to macroscopic order induced by the static electric field in the entire sample. HRS is more widely applicable for determination of  $\beta$  since macroscopic order in the sample is not required. However, HRS is sensitive to microscopic order since orientational correlations can result in the coherent addition of scattered light from a group of molecules. The measured HRS intensity is related to an effective molecular hyperpolarizability by  $I^{2\omega} \propto F\beta^2$ , where  $F$  accounts for the other sample-dependent factors and is given by<sup>7</sup>

$$F = \frac{\rho \mathcal{L}^A \mathcal{L}^2 T_\omega^2 T_{2\omega} n_\omega}{n_{2\omega}^2}. \quad (4)$$

In this equation  $\rho$  is the molecular number density,  $n$  is the sample refractive index,  $\mathcal{L}$  is the Lorentz local field factor, and  $T$  is the Fresnel transmission factor.

Relative values of  $\beta$  are obtained by comparing HRS measurements of  $(I^{2\omega}/F)^{1/2}$  obtained from different samples in the same apparatus. Combining HRS intensity measurements for vapor and liquid samples determines the ratio  $\beta_L/\beta_G$ , where  $\beta_L$  is the effective hyperpolarizability of molecules in the liquid phase, and  $\beta_G$  is the hyperpolarizability of the same molecules in the gas phase. The ratio  $\beta_L/\beta_G$  is a direct measure of the influence of the liquid environment on the value of  $\beta$ .

Absolute values of  $\beta_L$  for molecules in the liquid are obtained from HRS relative intensity measurements combined with gas-phase EFISH results, using the expression

$$\beta_L = \left(\frac{\beta_L}{\beta_G}\right)^{\text{HRS}} \left(\frac{\beta_{\text{HRS}}}{\beta_{\parallel}}\right)^{\text{theory}} (\beta_{\parallel})_G^{\text{EFISH}}. \quad (5)$$

Equation (5) also requires an independent assessment of the ratio of the hyperpolarizabilities,  $\beta_{\text{HRS}}/\beta_{\parallel}$ . When *ab initio* calculations for all the tensor elements of  $\beta$  are available, we can use the theoretical results to evaluate the explicit expressions<sup>8,9</sup> for this ratio for molecules of  $C_{2v}$  and  $C_{3v}$  symmetry. The ratio  $\beta_{\text{HRS}}/\beta_{\parallel}$  is adequately known from *ab initio* calculations for chloroform,<sup>10</sup> acetonitrile,<sup>11</sup> and water.<sup>12</sup> When less complete information is available, and  $\beta$  is dominated by  $\beta_{zzz}$ , it is a good approximation to use the expression for the case of  $C_{\infty v}$  symmetry. In this case, and for HRS measurements in the VV polarization geometry,  $\beta_{\text{HRS}}$  is given by

$$\beta_{\text{HRS}}^2 \equiv \langle \beta_{zzz}^2 \rangle = \frac{1}{35} (5\beta_{zzz}^2 + 12\beta_{zzz}\beta_{zxx} + 24\beta_{zxx}^2), \quad (6)$$

Figure 1 shows  $\beta_{\parallel}/\beta_{\text{HRS}}$  plotted as a function of  $\beta_{zxx}/\beta_{zzz}$  using Eqs. (3) and (6) for the case of  $C_{\infty v}$  symmetry. If only  $\beta_{zzz} \neq 0$ , then  $\beta_{\parallel}/\beta_{\text{HRS}} = 3\sqrt{7}/5 \approx 1.59$  for  $C_{2v}$ ,  $C_{3v}$ , and  $C_{\infty v}$  symmetry. For para-nitroaniline (pNA) and nitroben-

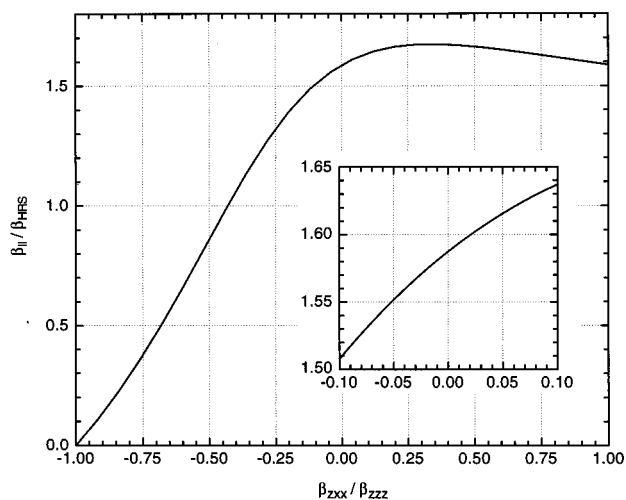


FIG. 1. The hyperpolarizability ratio,  $\beta_{\parallel}/\beta_{\text{HRS}}$ , as calculated from Eqs. (3) and (6) for HRS measurements in the VV polarization geometry, as a function of the value of  $R = \beta_{zxx}/\beta_{zzz}$  for  $C_{\infty v}$  symmetry. The inset shows the relation between the hyperpolarizability ratio  $\beta_{\parallel}/\beta_{\text{HRS}}$  and values of  $R$  in an expanded scale near  $R = 0$ .

zene we have used dilute solution HRS polarization measurements<sup>3</sup> to determine the ratio of the largest tensor components in order to evaluate  $\beta_{\text{HRS}}/\beta_{\parallel}$ . For methanol and nitromethane, *ab initio* calculations were not available and dilute solution HRS polarization measurements were not possible, so we have used the approximation valid for the case of  $C_{\infty v}$  symmetry,  $\beta_{\parallel}/\beta_{\text{HRS}} = 3\sqrt{7}/5 \approx 1.59$ .

As a check of the accuracy of the  $\beta_L$  values obtained by the above procedure, we can use each  $\beta_L$  value to calibrate an independent HRS determination of  $\beta_L$  for  $\text{CCl}_4$ . To do this, the  $\beta_L$  value for each molecule  $X$  is combined with liquid HRS intensity ratio measurements for molecule  $X$  and for  $\text{CCl}_4$  using the expression

$$\beta_L^{\text{CCl}_4} = \beta_L^X \left( \frac{I_{\text{CCl}_4} F_X}{F_{\text{CCl}_4} I_X} \right)_L^{1/2}. \quad (7)$$

The independent determinations of  $\beta_L$  for  $\text{CCl}_4$  should all agree. As a further test,  $\beta_{xyz}$  of  $\text{CCl}_4$  in the gas phase can be determined using the expression

$$\beta_{xyz}^{\text{CCl}_4} = \sqrt{\frac{35}{12}} \left( \frac{\beta_G}{\beta_L} \right)_{\text{CCl}_4}^{\text{HRS}} \beta_L^{\text{CCl}_4}. \quad (8)$$

The value so obtained for  $\beta_{xyz}$  of  $\text{CCl}_4$  in the gas phase may be compared with the result previously obtained by an analysis of the liquid  $\text{CCl}_4$  HRS spectrum.<sup>5</sup>

### III. EXPERIMENT

The molecules investigated in this work are listed in Tables I–III. Hydrogenated compounds were obtained from Aldrich Chemical (spectroscopic grade), except for para-nitroaniline (pNA) which was obtained from Chromophore Inc., and for the deuterated molecules which were obtained

TABLE I. EFISH data for phase-match densities and hyperpolarizabilities at  $\lambda_\omega = 1064$  nm. Typical phase-match densities of  $N_2$  were about  $\rho \approx 86 \text{ mol/m}^3 = 1.93 \text{ Loschmidts No./cm}^3$ . The mixed gas samples contained approximately mole fraction  $X$  of vapor. The reference value for the second hyperpolarizability of  $N_2$  at 1064 nm is  $\gamma = 964.5 \pm 3 \text{ au}$  (Ref. 13).

Molecule	$X$ (%)	$T$ ( $^\circ\text{C}$ )	$\rho_{N_2}/\rho_X$	$\Gamma_X/\gamma_{N_2}$
CCl <sub>4</sub>	2.7	94.2	9.41±0.06	12.82±0.21
	2.6	199.7	9.44±0.09	12.77±0.17
CDCl <sub>3</sub>	3.2	25.7	8.01±0.05	12.19±0.10
	3.2	120.2	8.04±0.05	12.10±0.18
	2.6	199.5	7.89±0.09	12.21±0.21
CH <sub>3</sub> CN	3.3	30.3	3.75±0.02	14.61±0.10
	3.3	39.5	3.72±0.01	13.87±0.02
	3.0	78.7	3.77±0.01	13.16±0.04
	2.8	127.8	3.76±0.02	11.88±0.18
	2.7	195.8	3.76±0.03	10.93±0.15
CD <sub>3</sub> CN	3.3	39.2	3.67±0.01	14.55±0.12
	3.2	49.4	3.68±0.01	14.18±0.08
	3.1	68.9	3.67±0.02	14.03±0.11
	3.0	157.4	3.71±0.07	11.97±0.10
	2.8	196.9	3.69±0.01	11.28±0.12
CH <sub>3</sub> OD	2.8	32.6	2.57±0.06	-3.60±0.06
	2.5	88.3	2.57±0.04	-2.52±0.06
	2.6	159.6	2.62±0.04	-1.41±0.10
	2.4	191.8	2.53±0.07	-1.05±0.13
CD <sub>3</sub> NO <sub>2</sub>	1.6	31.5	5.40±0.09	-11.69±0.28
	1.4	90.0	5.37±0.05	-8.99±0.12
	1.7	141.6	5.43±0.08	-7.55±0.16
	2.1	200.0	5.36±0.08	-5.66±0.15
D <sub>2</sub> O	4.0	57.7	1.19±0.02	-2.47±0.07
	4.2	88.4	1.21±0.01	-2.16±0.11
	4.5	154.4	1.20±0.02	-1.57±0.09
	5.2	202.7	1.24±0.02	-1.19±0.06
H <sub>2</sub> O	2.9	58.7	1.31±0.02	-2.73±0.05
	4.1	73.5	1.36±0.02	-2.64±0.07
	4.8	109.5	1.35±0.04	-2.19±0.03
	5.0	131.7	1.33±0.01	-1.88±0.08
	4.7	161.6	1.35±0.02	-1.72±0.05
	5.3	202.8	1.35±0.01	-1.35±0.04
C <sub>6</sub> H <sub>6</sub>	2.1	154.1	15.27±0.21	18.34±0.31
C <sub>6</sub> D <sub>6</sub>	2.0	200.0	15.52±0.14	18.44±0.19
C <sub>6</sub> H <sub>5</sub> NO <sub>2</sub>	0.26	84.4	23.88±0.20	121.0±1.1
	0.50	98.3	24.04±0.13	118.1±1.0
	0.43	157.2	24.19±0.18	104.4±0.8
	0.40	196.2	24.09±0.10	97.3±0.7
pNA <sup>a</sup>	0.075	196.9	42.4±1.4	737±19

<sup>a</sup>Para-nitroaniline.

from Cambridge Isotope Laboratories. All molecules were used as received except for pNA which was purified three times by recrystallization in methanol.

The experimental apparatus used in this work for both the EFISH and HRS measurements has been described in detail in previous publications.<sup>7,11,13</sup> An acousto-optically  $Q$ -switched Nd:YAG laser (Quantronix 116) provided the incident radiation at 1064 nm for both experiments. The laser

TABLE II. Results from gas-phase EFISH measurements calibrated with respect to the reference value for the second hyperpolarizability of  $N_2$  at 1064 nm,  $\gamma = 964.5 \pm 3 \text{ au}$  (Ref. 13). The hyperpolarizabilities are given in atomic units where:  $\beta = 1 \text{ au} = 3.20636 \times 10^{-53} \text{ C}^3 \text{ m}^3 \text{ J}^{-2} = 8.6392 \times 10^{-33} \text{ esu}$  and  $\gamma = 1 \text{ au} = 6.235377 \times 10^{-65} \text{ C}^4 \text{ m}^4 \text{ J}^{-3} = 5.0367 \times 10^{-40} \text{ esu}$ .

Molecule	$\mu(\text{D})^a$	$\gamma/\gamma_{N_2}$	$\beta_{  }$ (au)
CCl <sub>4</sub>	0	12.8±0.2	0
CDCl <sub>3</sub>	1.04	12.0±0.6	+1.0±4.2
CH <sub>3</sub> CN	3.92	4.41±0.58	+17.9±1.1
CD <sub>3</sub> CN	3.92	4.97±0.31	+17.7±0.8
CH <sub>3</sub> OD	1.70	3.87±0.20	-31.2±1.6
CD <sub>3</sub> NO <sub>2</sub>	3.46	4.87±0.56	-33.7±1.5
D <sub>2</sub> O	1.81	1.72±0.24	-17.8±1.2
H <sub>2</sub> O	1.85	1.87±0.17	-19.2±0.9
C <sub>6</sub> H <sub>6</sub>	0	18.4±0.3	0
C <sub>6</sub> D <sub>6</sub>	0	18.3±0.2	0
C <sub>6</sub> H <sub>5</sub> NO <sub>2</sub>	4.22	20.3±3.9	+197±9
pNA	6.87 <sup>b</sup>	60±30 <sup>c</sup>	+1072±44

<sup>a</sup>Reference 38. If unavailable, values for the deuterated molecules are assumed to be the same as the nondeuterated molecules.

<sup>b</sup>Reference 39.

<sup>c</sup>Reference 40.

was operated at a repetition rate of 1–7 kHz, where it produced trains of  $\approx 150$ –250 ns, 1 mJ pulses. The EFISH measurements were made by weakly focusing the laser through a periodic electrode array (61 mm period, 7 repeats) contained in a cylindrical gas cell.<sup>11,13</sup> Periodic phase matching and maximum signal occur when the coherence length of the gas in the cell matches the period of the electrode array. This condition is achieved by adjusting the gas pressure in the cell. Sample densities were calculated from the measured

TABLE III. Molecular hyperpolarizabilities obtained from gas-phase EFISH measurements in this work compared with previous gas-phase EFISH results.

Molecule	Wavelength (nm)	$\gamma$ (au)	$\beta_{  }$ (au)
CCl <sub>4</sub>	1064	12 350±190 <sup>a</sup>	
	694.3	16 480±240 <sup>b</sup>	
CHCl <sub>3</sub>	694.3	13 470±360 <sup>b</sup>	1.2±2.6 <sup>b</sup>
CDCl <sub>3</sub>	1064	11 570±580 <sup>a</sup>	1.0±4.2 <sup>a</sup>
H <sub>2</sub> O	1064	1 800±150 <sup>a</sup>	-19.2±0.9 <sup>a</sup>
	694.3	2 310±120 <sup>c</sup>	-22.0±0.9 <sup>c</sup>
D <sub>2</sub> O	1064	1 660±220 <sup>a</sup>	-17.8±1.2 <sup>a</sup>
CH <sub>3</sub> OH	694.3	4 590±130 <sup>c</sup>	-35.0±2.1 <sup>c</sup>
CH <sub>3</sub> OD	1064	3 730±190 <sup>a</sup>	-31.2±1.6 <sup>a</sup>
C <sub>6</sub> H <sub>6</sub>	1064	17 750±190 <sup>a</sup>	
	694.3	23 810±460 <sup>d</sup>	
	694.3	24 780±600 <sup>e</sup>	

<sup>a</sup>This work.

<sup>b</sup>Reference 15.

<sup>c</sup>Reference 17.

<sup>d</sup>References 18, 19, and this work, interpolated from the dispersion curve, see Fig. 5.

<sup>e</sup>Reference 16.

pressures and temperatures using the virial equation of state.<sup>11,14</sup> The hyperpolarizability of the sample gas was determined by comparing the harmonic signal for a mixture of sample vapor and N<sub>2</sub> buffer gas with the harmonic signal for N<sub>2</sub> reference gas, for which an absolute value of the hyperpolarizability is available.<sup>13</sup> Reference measurements were performed before and after each sample measurement and typically three to five sample measurements were made at each temperature. The ratio of the phase match densities for N<sub>2</sub> gas and pure sample vapor ( $\rho_{N_2}/\rho_X$ ) were also determined.

Improvements to the previously reported EFISH apparatus<sup>11</sup> include better temperature stabilization and temperature uniformity of the sample cell in the enclosing oven, better sample preparation and mixing, and the use of an alternating voltage supply for the electrode array. The preparation of sample mixtures with accurately known composition is critically important but difficult. The phase match density ratio is a useful diagnostic for mixture reproducibility, but does not provide an absolute assay. In the cases of the dilute vapor mixtures of pNA and nitrobenzene, where the mixing problem is most acute, the mixture composition was assayed by *in situ* UV absorption measurements calibrated against similar measurements of the pure vapor. This assay was used to develop and test an adequate mixing procedure for the other gases. An alternating electrode array voltage is preferred over a constant voltage, since then the second-harmonic generation (SHG) signal generated in the sample and that generated elsewhere in the apparatus add in quadrature. This eliminates a potential systematic error in the measurements due to interference between unwanted SHG light and the SHG signal from the sample. The dead time correction expression is slightly more complicated in the case of a sinusoidally varying electrode voltage than was the previous expression for the case of constant electrode voltage.<sup>13</sup> Typically, the voltage applied to the EFISH cell was set so that the second-harmonic signal with a 3 kHz laser pulse repetition rate was about 600 counts/s at the phase match density.

In the HRS measurements, the second-harmonic scattered light was collected at 90° in the VV polarization geometry with  $f/2.1$  optics and focused into a spectrometer (Jobin–Yvon Ramanor U 1000), with polarization selection by a sheet polaroid.<sup>7</sup> The measurements were made by placing  $\approx 1$  cm<sup>3</sup> for the filtered (0.2  $\mu$ m) sample liquid in a standard 1 cm spectroscopic cuvette. The scattering from the liquid and from the vapor can be compared by simply shifting the cuvette vertically a few millimeters so that the laser beam passes either through the liquid or just above the liquid surface. The liquid-phase intensity was measured at 22 °C, but the sample cell was heated to raise the vapor pressure for the gas-phase measurement. A valid comparison of liquid and vapor scattering intensities requires that the scattering and collection geometry be correctly set for both samples, as previously described.<sup>7</sup> The spectrometer slits were opened up to a spectral slit width of 25 cm<sup>-1</sup> when the HRS intensities of liquid- and gas-phase samples were being compared, but narrower slits were employed when liquid samples were

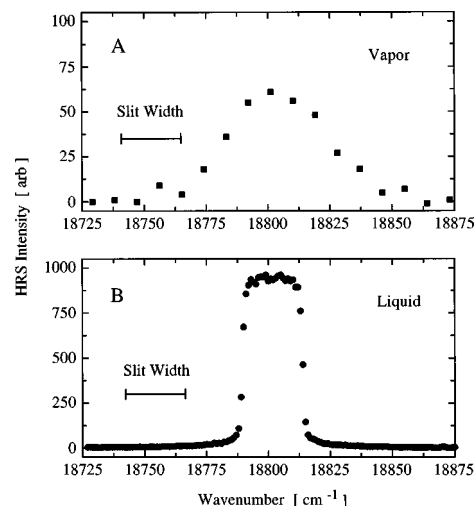


FIG. 2. Comparison of the HRS spectra of nitrobenzene in the (A) gas phase and (B) liquid phase, observed in the VV polarization geometry. The gas phase spectrum was collected at  $101 \pm 2$  °C, with the spectrometer spectral slit width set at 25 cm<sup>-1</sup>. The rotational line and branch structure is unresolved, but the band is only slightly instrumentally broadened. The liquid phase spectrum was collected at 22 °C with 25 cm<sup>-1</sup> spectral slit width. The gas-phase rotational structure collapses to a narrow band with weak broad wings in the liquid (bandwidth <2 cm<sup>-1</sup>).

compared. Care was taken to correct for the effects of beam absorption and thermal lensing for the liquid HRS measurements. Figure 2 shows the gas- and liquid-phase HRS spectra for nitrobenzene. Low signal levels and the consequently wide spectral slit width prevented any detailed resolution of the features of the gas-phase spectrum. The second-harmonic scattered light was detected by a cooled photon counting photomultiplier tube (Hamamatsu R943) and data collection was accomplished with a multichannel scaler (Nucleus PCA). The effective value of  $\beta$  is then simply obtained from the integrated intensity of the second-harmonic signal. Typically  $10^4$ – $10^5$  counts from second-harmonic photons were obtained in the liquid-phase measurements, whereas only about 200–1000 counts were obtained in the gas-phase measurements.

#### IV. RESULTS AND DISCUSSION

The gas-phase EFISH results for the molecules investigated in this work are presented in Tables I and II and Figs. 3–5. The hyperpolarizability ratios plotted in Figs. 3 and 4 show the linear variation with  $1/T$  predicted by Eq. (2). The relative first and second hyperpolarizabilities of each molecule are obtained from the slope and intercept of the least-squares fit of a straight line to the values of  $\Gamma$  plotted vs  $1/T$ . The absolute values of the hyperpolarizabilities are extracted from the measured ratios using the previously determined value  $\gamma = 964.5 \pm 3$  au at  $\lambda = 1064$  nm for N<sub>2</sub>.<sup>13</sup> The accuracy of the  $\Gamma$  measurements is typically about 1%, but the limited temperature range of the measurements results in magnified uncertainties for the slope and intercept of the fitted lines. With the exception of chloroform, typical statistical uncertainties are about  $\pm 5\%$  for  $\beta_{\parallel}$  and  $\pm 5\%$ – $15\%$  for  $\gamma$ . For several of the molecules, both normal and deuterated versions were measured. Figure 3 shows a clear upward shift

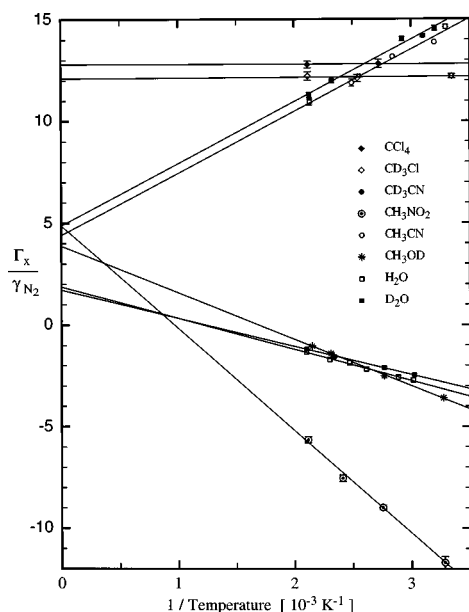


FIG. 3. A plot of the hyperpolarizability ratios  $\Gamma_X/\gamma_{N_2}$  vs the inverse temperature. The relative first and second hyperpolarizabilities of each molecule are obtained from the slope and intercept of the least-squares fit of a straight line. The absolute values of the hyperpolarizabilities are extracted from the measured ratios using the previously determined value of  $\gamma_{N_2}$  (964.5 au at 1064 nm) (Ref. 13). The molecules are listed in decreasing order of the value of the intercept of  $\Gamma_X/\gamma_{N_2}$  for each molecule.

of  $\Gamma$  for acetonitrile and water upon deuteration, but the differences between the fitted values of  $\beta_{||}$  and  $\gamma$  for the normal and deuterated molecules are, at most, marginally significant (e.g.,  $-1.4 \pm 1.5$  au for  $\beta_{||}$  of water, and  $-540 \pm 630$  au for  $\gamma$  of acetonitrile).

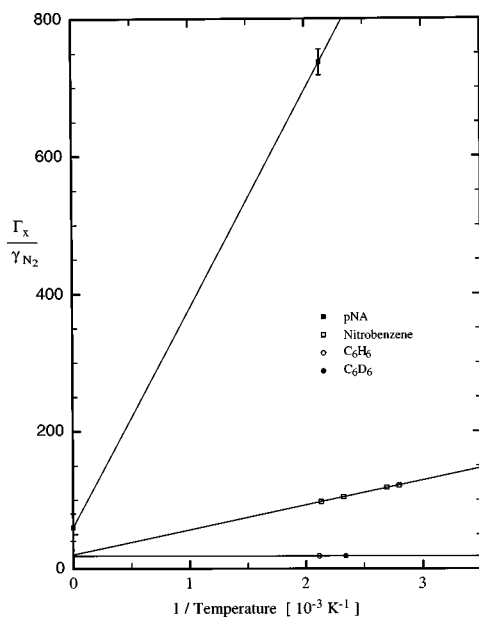


FIG. 4. A plot of the hyperpolarizability ratios  $\Gamma_X/\gamma_{N_2}$  vs the inverse temperature for the molecules pNA, nitrobenzene, and benzene, as in Fig. 2. The intercept for pNA is from a dilute solution THG measurement (Ref. 40).

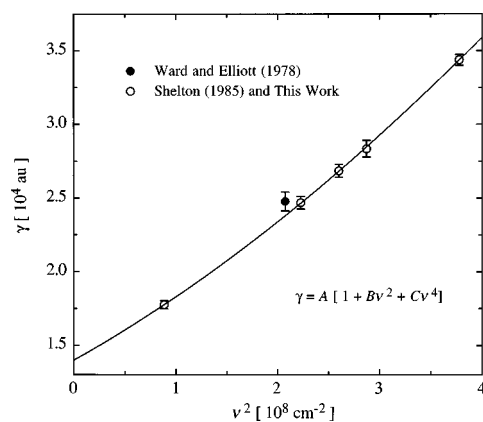


FIG. 5. Dispersion of the second hyperpolarizability of benzene from gas-phase EFISH measurements. A weighted least-squares fit of the function  $\gamma = A[1 + B\nu^2 + C\nu^4]$  to the previous results of Refs. 18 and 19, and the present datum at 1064 nm, gives values of  $A = 13980$  au,  $B = 2.81 \times 10^{-9}$  cm<sup>2</sup>, and  $C = 2.77 \times 10^{-18}$  cm<sup>4</sup>. The results of Ref. 16 at 694.3 nm are about 4% higher than the interpolated result from our dispersion curve.

Table III provides a comparison of the present results with the results of previous EFISH measurements by Ward *et al.* for some of the same molecules.<sup>15-17</sup> A detailed comparison of the present results with the results of Ward *et al.* is warranted because those results have been so widely adopted. The results of the two experiments disagree by more than the combined error bars, but this could be simply due to the measurements being made at different wavelengths. The effect of frequency dispersion can be assessed in the case of benzene by combining the results of this work with data at several additional wavelengths, as shown in Fig. 5. The additional data were previously obtained by Shelton<sup>18,19</sup> with an apparatus and techniques similar to that used in the present measurements. The result for benzene from Ward *et al.* falls 4% above the fitted dispersion curve in Fig. 5; this curve indicates that  $\gamma$  for benzene at 694.3 nm is 34% higher than at 1064 nm. The value for  $\gamma$  of  $\text{CCl}_4$  at 1064 in Table III can also be reconciled with the measured value of  $\gamma$  at 694.3 nm if one assumes the same  $\approx 34\%$  dispersion as for benzene. Similar results are obtained for the dipolar molecules. For  $\gamma$  the values at 694.3 nm are 1.16–1.40 times larger than those at 1064 nm, while for  $\beta_{||}$  the values are 1.07–1.14 times larger. These differences can probably also be accounted for by the frequency dependence of the hyperpolarizabilities.

Table IV shows the results obtained from HRS measurements for several molecules. The direct HRS measurements in columns 4 and 5 have been combined with the EFISH results in Table II, using Eqs. (4), (5), and (7) to obtain the  $\beta_L$  values in the final two columns of Table IV. The multiple independent determinations of  $\beta_L$  for  $\text{CCl}_4$  shown in the second to last column of Table IV test the consistency of the experimental results. All of these values of  $\beta_L$  for  $\text{CCl}_4$ , except for the one obtained from the chloroform data, agree to well within their error bars. The good agreement of these independent determinations shows that all the experimental results are consistent, and rules out significant sample-

TABLE IV. Results of liquid- and gas-phase HRS measurements in the VV polarization geometry at  $\lambda_\omega = 1064$  nm. The liquid measurements were done at  $22 \pm 1$  °C. The agreement of the values in the second to last column is a measure of the consistency of the experimental results for the various molecules (see the text). The final column contains the best  $\beta_L$  value determined for each molecule based on the HRS intensity ratio  $I_X/I_{\text{CCl}_4}$  and the weighted average of the values for  $\beta_L^{\text{CCl}_4}$ .

Molecule	$F(M)^a$	$\beta_{\parallel}/\beta_{\text{HRS}}$	$\beta_L/\beta_G$	$I_X/I_{\text{CCl}_4}$	$\beta_L^{\text{CCl}_4}(\text{au})$	$\beta_L^X(\text{au})$
CCl <sub>4</sub>	46.8	0	$1.53 \pm 0.10$	1.00		$18.6 \pm 0.6^b$
CDCl <sub>3</sub>	53.6	$0.96 \pm 0.30^c$	$1.70 \pm 0.10$	$0.82 \pm 0.02$	$2 \pm 12$	$15.7 \pm 0.7$
CH <sub>3</sub> CN	57.8	$1.65 \pm 0.02^d$	$1.90 \pm 0.10$	$1.65 \pm 0.05$	$17.8 \pm 1.4$	$21.4 \pm 0.9$
CD <sub>3</sub> CN	57.8	$1.65 \pm 0.02^d$	$2.00 \pm 0.10$	$1.70 \pm 0.05$	$18.3 \pm 1.3$	$21.8 \pm 0.9$
CH <sub>3</sub> OD	70.4	$1.59 \pm 0.05^e$	$0.41 \pm 0.04$	$0.25 \pm 0.02$	$19.5 \pm 2.7$	$7.5 \pm 0.4$
CD <sub>3</sub> NO <sub>2</sub>	63.7	$1.59 \pm 0.05^e$	$0.52 \pm 0.05$	$0.38 \pm 0.03$	$20.8 \pm 2.7$	$9.8 \pm 0.5$
D <sub>2</sub> O	160.4	$1.70 \pm 0.02^f$	$0.81 \pm 0.08$	$0.59 \pm 0.03$	$20.5 \pm 2.6$	$7.7 \pm 0.4$
C <sub>6</sub> H <sub>5</sub> NO <sub>2</sub>	58.1	$1.63 \pm 0.01^g$	$1.30 \pm 0.10$	$95 \pm 5$	$18.0 \pm 1.7$	$162 \pm 8$
pNA		$1.58 \pm 0.01^g$				

<sup>a</sup>Calculated from Eq. (4) using data from Ref. 41.

<sup>b</sup>Calculated based on the weighted average of the results given in the previous column for  $\beta_L^{\text{CCl}_4}$ , excluding the result from CDCl<sub>3</sub>.

<sup>c</sup>Calculated from Ref. 10.

<sup>d</sup>Calculated from Ref. 11.

<sup>e</sup>Calculated assuming only  $\beta_{zzz} \neq 0$ , see Fig. 1.

<sup>f</sup>Calculated from Ref. 12.

<sup>g</sup>Calculated from dilute solution HRS polarization measurements.

specific systematic errors. The results shown in the last column of Table IV are our best estimates of  $\beta_L$  for each molecule. The result for CCl<sub>4</sub> is obtained using the weighted average of the  $\beta_L$  values for CCl<sub>4</sub> in the second to last column; this effectively combines all the gas-phase EFISH  $\beta_{\parallel}$  measurements to improve the accuracy of the calibration. This  $\beta_L$  value for CCl<sub>4</sub> is then used in Eq. (7) as the common reference standard for the liquid HRS measurements. This gives HRS  $\beta_L$  values most accurately calibrated in terms of gas-phase EFISH  $\beta_{\parallel}$  measurements. A final check of the accuracy of the present experimental results is obtained when Eq. (8) is used to obtain  $\beta_{xyz}$  for CCl<sub>4</sub> from the best estimate of the value of  $\beta_L$  for CCl<sub>4</sub>. The result is  $\beta_{xyz} = 20.7 \pm 1.6$  au, which is in reasonable agreement with  $\beta_{xyz} = 19$  au obtained previously in a less direct way from an analysis of CCl<sub>4</sub> liquid- and vapor-phase HRS spectra.<sup>5</sup> Thus, all indications are that the present experimental results are consistent and accurate to within the stated error bars.

The values of  $\beta_L/\beta_G$  given in the fourth column of Table IV show that the effective  $\beta$  of these molecules in the liquid is enhanced over the gas-phase value by a factor which

varies from 0.4 to 2.0. The molecules with negative  $\mu\beta_{\parallel}$  have  $\beta_L < \beta_G$ . Our previous study of CCl<sub>4</sub> HRS spectra has identified two main intermolecular interaction effects which modify  $\beta$  in the liquid.<sup>5</sup> They are: (1) orientational correlations between neighboring molecules and (2) distortion of a molecule by the permanent multipolar fields of its neighbors. For CCl<sub>4</sub>, the unimolecular, orientational correlation, and multipolar contributions to the liquid HRS intensity are all comparable (approximately 40%, 20%, 40%, respectively). The interaction effects are even larger for some of the other small molecules in Table IV, but the relative importance of the orientational correlations as compared to the multipolar fields for these molecules is at present unknown. Further study is needed to disentangle the effects. If the multipolar field contributions were ignorable, then the increase in  $\beta$  for acetonitrile molecules in the liquid would indicate net parallel orientational correlations between neighbors, while the decrease in  $\beta$  for methanol would indicate net antiparallel orientational correlations. Because EFISH measurements are insensitive to short-range orientational correlations, liquid EFISH and HRS results may be expected to differ when

TABLE V. First hyperpolarizability  $\beta_{\parallel}$  values of CHCl<sub>3</sub> from various experimental measurements and theoretical calculations.

Wavelength (nm)	$\beta_{\parallel}$ (au)	Method	Reference
1064	$+1.0 \pm 4.2$	Gas-phase EFISH	This Work
694.3	$+1.2 \pm 2.6$	Gas-phase EFISH	15
694.3	+92	Gas-phase EFISH	42
1064	$-68 \pm 7$	Liquid-phase EFISH	29 <sup>a</sup>
694.3	+90	EFISH+TWM	15
632.8	$-156 \pm 125$	Kerr effect	43
694.3	-10.2	CHF	10
694.3	-1.4	MP2	44

<sup>a</sup>Calibration requires  $\chi^{(2)}$  of quartz and  $\chi^{(3)}$  of fused silica and CHCl<sub>3</sub>.

TABLE VI. First hyperpolarizability  $\beta_{||}$  values of H<sub>2</sub>O from various experimental measurements and theoretical calculations.

Wavelength (nm)	$\beta_{  }$ (au)	Method	Reference
1064	-19.2±0.9	Gas-phase EFISH	This work
694.3	-22.0±0.9	Gas-phase EFISH	17
1064	+19.2	Liquid-phase EFISH	45 <sup>a</sup>
Static	-11.0	SCF	33
Static	-17.3	MP2	33
Static	-16.8	SDQ MP4	33
Static	-24.8	DFT LDA	46
1064	-13.1	MCSCF	34
694.3	-20.8	MCSCF	35
694.3	-19.6	DFT LDA	47
694.3	-21.1	CCSD(T)	12

<sup>a</sup>Calibration requires  $\chi^{(2)}$  of quartz and  $\chi^{(3)}$  of fused silica and H<sub>2</sub>O.

orientational correlations contribute significantly to the HRS signal.

The results given in Tables II and IV should be useful for accurately calibrating experimental measurements and testing theoretical calculations. Many of the available reference standards are in need of improvement. Chloroform has frequently<sup>20–28</sup> been used as a HRS reference standard in which the liquid-phase EFISH value measured by Kajzar *et al.*<sup>29</sup> is used to calibrate the HRS signals. This EFISH value for  $\beta_{||}$ , however, is dependent on the values of the nonlinear susceptibilities of quartz and glass, which are now believed<sup>30,31</sup> to be lower than the values used by Kajzar *et al.* In Table V we compare values of the first hyperpolarizability  $\beta_{||}$  of chloroform from various experimental measurements and theoretical calculations. It is evident that there are wide discrepancies between the various published values, much larger than can be attributed to frequency dependence, vibrational contributions, isotopic substitution, or intermolecular interactions. Even given an accurate EFISH value of  $\beta_{||}$  for chloroform, the liquid HRS calibration based on  $\beta_{||}$  may still be inaccurate because of the large effect of molecular interactions on  $\beta$  values obtained by HRS. Note that chloroform is the only dipolar molecule in the present study for which the EFISH measurement does not give a reliable calibration of the HRS  $\beta$  for the same molecule (see Table IV). An additional technical consideration bearing on the use of pure solvents for HRS calibration is that they can be particularly susceptible to parasitic HRS from incompletely filtered samples, leading to an overestimation of the corresponding first hyperpolarizabilities,<sup>32</sup> though this has not been a problem with our apparatus.

A comparison of experimental measurements and theoretical calculations of the first hyperpolarizability  $\beta_{||}$  of H<sub>2</sub>O is presented in Table VI. The water molecule is an especially interesting case because it is small enough that accurate theoretical results should be feasible and many calculations have been performed. The results of *ab initio* calculations at the self-consistent field (SCF) level are consistently below the experimental values for  $\beta$ . This is probably due to electron correlation effects since the largest basis sets used appear adequate to have reached the SCF limit for the calcu-

lated value of  $\beta$ .<sup>33</sup> Inclusion of electron correlation results in  $\beta$  values which are more widely scattered, but which tend to fall near the experimental result obtained in this work.<sup>34,35</sup> Vibrational contributions are not included in any of the calculated values given in Table VI. Luo *et al.*<sup>35</sup> estimate that zero point vibrational averaging contributions at optical frequencies are about 10% of the value of  $\beta_{||}$ , while Bishop *et al.*<sup>36</sup> conclude that pure vibrational contributions are less than 2% of the total value. The difference between the experimental values of  $\beta_{||}$  for H<sub>2</sub>O and D<sub>2</sub>O gives a rough indication of the size of the vibrational contribution; the difference is 8% ± 12%, consistent with these theoretical estimates. Such comparisons with the available experimental measurements indicate that present algorithms used to calculate *ab initio* hyperpolarizability values of small polyatomic molecules give results which are at about the 10% level of accuracy.<sup>37</sup>

## V. CONCLUSIONS

One motivation for the present study was a need for reference standards for HRS measurements, and so appropriate molecular hyperpolarizability values  $\beta$  were determined for several molecules. We conclude that CCl<sub>4</sub> is well suited for a reference standard, although for routine use pNA will probably be preferred, due to the higher HRS signals available. Our own preference is to calibrate the HRS signal from pNA with respect to CCl<sub>4</sub> and then use solutions of pNA as a secondary reference.<sup>3</sup> A second objective of this study was to measure and compare  $\beta$  in the liquid and gas phases. It is found that the effective HRS  $\beta$  is increased or decreased by as much as a factor of 2 due to intermolecular interactions and orientational correlations between neighboring molecules in the liquid phase. A third objective was to probe vibrational contributions to the hyperpolarizabilities by comparing results for hydrogenated and deuterated molecules. The effect of deuteration is small for  $\beta$  (≤ 5%) but somewhat larger for  $\gamma$  (≤ 10%).

*Note added in proof.* Recent work<sup>48</sup> calls into question the usual local field factors for nonlinear optics experiments,

and the hyperpolarizabilities of molecules in the liquid phase may need re-examination.

## ACKNOWLEDGMENT

This work was partially supported by the DOE under Grant No. DE-FG02-91ER75667.

- <sup>1</sup>K. Clays, A. Persoons, and L. De Maeyer, in *Advances in Chemical Physics*, edited by M. Evans and S. Kielich (Wiley, New York, 1994), Vol. 85, p. 455.
- <sup>2</sup>J. Zyss and I. Ledoux, *Chem. Rev.* **94**, 77 (1994).
- <sup>3</sup>P. Kaatz and D. P. Shelton, *J. Chem. Phys.* **105**, 3918 (1996).
- <sup>4</sup>A. Willetts, J. E. Rice, D. M. Burland, and D. P. Shelton, *J. Chem. Phys.* **97**, 7590 (1992).
- <sup>5</sup>P. Kaatz and D. P. Shelton, *Mol. Phys.* **88**, 683 (1996).
- <sup>6</sup>D. P. Shelton and J. E. Rice, *Chem. Rev.* **94**, 3 (1994).
- <sup>7</sup>P. Kaatz and D. P. Shelton, *Rev. Sci. Instrum.* **67**, 1438 (1996).
- <sup>8</sup>S. J. Cyvin, J. E. Rauch, and J. C. Decius, *J. Chem. Phys.* **43**, 4083 (1965).
- <sup>9</sup>R. Bersohn, Y. H. Pao, and H. L. Frisch, *J. Chem. Phys.* **45**, 3184 (1966).
- <sup>10</sup>S. P. Karna and M. Dupuis, *Chem. Phys. Lett.* **171**, 201 (1990).
- <sup>11</sup>M. Stählerin, C. R. Moylan, D. M. Burland, A. Willetts, J. E. Rice, D. P. Shelton, and E. A. Donley, *J. Chem. Phys.* **98**, 5595 (1993).
- <sup>12</sup>H. Sekino and R. J. Bartlett, *J. Chem. Phys.* **98**, 3022 (1993).
- <sup>13</sup>D. P. Shelton, *Phys. Rev. A* **42**, 2578 (1990).
- <sup>14</sup>J. Dymond and E. Smith, *The Virial Coefficients of Pure Gases and Mixtures* (Clarendon, Oxford, 1980).
- <sup>15</sup>C. K. Miller and J. F. Ward, *Phys. Rev. A* **16**, 1179 (1977).
- <sup>16</sup>J. F. Ward and D. S. Elliott, *J. Chem. Phys.* **69**, 5438 (1978).
- <sup>17</sup>J. F. Ward and C. K. Miller, *Phys. Rev. A* **19**, 826 (1979).
- <sup>18</sup>D. P. Shelton, *J. Opt. Soc. Am. B* **2**, 1880 (1985).
- <sup>19</sup>D. P. Shelton, *Chem. Phys. Lett.* **121**, 69 (1985).
- <sup>20</sup>K. Clays and A. Persoons, *Phys. Rev. Lett.* **66**, 2980 (1991).
- <sup>21</sup>G. J. T. Heesink, A. G. T. Ruiter, N. F. van Hulst, and B. Bölger, *Phys. Rev. Lett.* **71**, 999 (1993).
- <sup>22</sup>T. Verbiest, K. Clays, C. Samyn, J. Wolff, D. Reinhoudt, and A. Persoons, *J. Am. Chem. Soc.* **116**, 9320 (1994).
- <sup>23</sup>M. A. Pauley, C. H. Wang, and A. K. Y. Jen, *J. Chem. Phys.* **102**, 6400 (1995).
- <sup>24</sup>M. C. Flipse, R. Jonge, R. H. Woudenberg, A. W. Marsman, C. Walree, and L. W. Jenneskens, *Chem. Phys. Lett.* **245**, 297 (1995).
- <sup>25</sup>E. Hendrickx, K. Clays, A. Persoons, C. Dehu, and J. L. Brédas, *J. Am. Chem. Soc.* **117**, 3547 (1995).
- <sup>26</sup>Y. Luo, A. Cesar, and H. Ågren, *Chem. Phys. Lett.* **252**, 389 (1996).
- <sup>27</sup>S. Stadler, G. Bourhill, and C. Bräuchle, *J. Phys. Chem.* **100**, 6927 (1996).
- <sup>28</sup>O. F. J. Noordman and N. F. van Hulst, *Chem. Phys. Lett.* **253**, 145 (1996).
- <sup>29</sup>F. Kajzar, I. Ledoux, and J. Zyss, *Phys. Rev. A* **36**, 2210 (1987).
- <sup>30</sup>D. A. Roberts, *IEEE J. Quantum Electron.* **QE 28**, 2057 (1992).
- <sup>31</sup>A. Mito, K. Hagimoto, and C. Takahashi, *Nonlinear Opt.* **13**, 3 (1995).
- <sup>32</sup>I. D. Morrison, R. G. Denning, W. M. Laidlaw, and M. A. Stammers, *Rev. Sci. Instrum.* **67**, 1445 (1996).
- <sup>33</sup>G. Maroulis, *J. Chem. Phys.* **94**, 1182 (1991).
- <sup>34</sup>E. K. Dalskov, H. J. Aa. Jensen, and J. Oddershede, *Mol. Phys.* **90**, 3 (1997).
- <sup>35</sup>Y. Luo, H. Ågren, O. Vahtras, P. Jørgensen, V. Spirko, and H. Hettema, *J. Chem. Phys.* **98**, 7159 (1993).
- <sup>36</sup>D. M. Bishop, B. Kirtman, H. A. Kurtz, and J. E. Rice, *J. Chem. Phys.* **98**, 8024 (1993).
- <sup>37</sup>R. J. Bartlett and H. Sekino, in *Nonlinear Optical Materials: Theory and Modeling*, ACS Symposium Series No. **628**, edited by S. P. Karna and A. T. Yeates (American Chemical Society, Washington, DC, 1996), p. 23.
- <sup>38</sup>*Handbook of Chemistry and Physics*, 77th ed., edited by R. W. Weast (Chemical Rubber, Boca Raton, FL, 1996); *Encyclopedia of Chemical Technology*, 4th ed., edited by J. I. Kroschwitz (Wiley, New York, 1993), Vol. 8.
- <sup>39</sup>F. Sim *et al.*, *J. Phys. Chem.* **97**, 1158 (1993).
- <sup>40</sup>L.-T. Cheng *et al.*, *J. Phys. Chem.* **95**, 10631 (1991); corrected with the results of A. Mito *et al.*, *Nonlinear Opt.* **13**, 3 (1995).
- <sup>41</sup>J. Timmermans, *Physics-Chemical Constants of Pure Organic Compounds* (Elsevier, New York, 1950).
- <sup>42</sup>G. Hauchecorne *et al.*, *J. Phys. (Paris)* **32**, 47 (1971).
- <sup>43</sup>M. P. Bogaard *et al.*, *J. Chem. Soc. Faraday Trans.* **74**, 1573 (1978).
- <sup>44</sup>B. L. Hammond and J. E. Rice (unpublished); see *Chem. Rev.* **94**, 3 (1994).
- <sup>45</sup>B. F. Levine and C. G. Bethea, *J. Chem. Phys.* **65**, 2429 (1976).
- <sup>46</sup>R. M. Dickson and A. D. Becke, *J. Phys. Chem.* **100**, 16105 (1996).
- <sup>47</sup>J. Guan *et al.*, *J. Chem. Phys.* **98**, 4753 (1993).
- <sup>48</sup>R. Wortmann and D. M. Bishop, *J. Chem. Phys.* **108**, 1001 (1998), this issue.